

Original Article

Exposure to fine airborne particulate matter induces macrophage infiltration, unfolded protein response, and lipid deposition in white adipose tissue

Roberto Mendez¹, Ze Zheng¹, Zhongjie Fan⁵, Sanjay Rajagopalan³, Qinghua Sun^{3,4}, Kezhong Zhang^{1,2}

¹Center for Molecular Medicine and Genetics, ²Department of Immunology and Microbiology, Wayne State University School of Medicine, Detroit, MI 48201, USA; ³Division of Cardiovascular Medicine, Davis Heart and Lung Research Institute, College of Medicine, ⁴Division of Environmental Health Sciences, College of Public Health, Ohio State University, Columbus, OH 43210, USA; ⁵Department of Cardiology, Peking Union Medical College Hospital, Chinese Academy of Medical Science and Peking Union Medical College, Beijing, China

Received December 17, 2012; Accepted February 15, 2013; Epub March 28, 2013; Published April 8, 2013

Abstract: Recent epidemiological studies have suggested a link between exposure to ambient air-pollution and susceptibility to metabolic disorders such as Type II diabetes mellitus. Previously, we provided evidence that both short- and long-term exposure to concentrated ambient particulate matter with aerodynamic diameter $<2.5 \mu\text{m}$ ($\text{PM}_{2.5}$) induces multiple abnormalities associated with the pathogenesis of Type II diabetes mellitus, including insulin resistance, visceral adipose inflammation, brown adipose mitochondrial adipose changes, and hepatic endoplasmic reticulum (ER) stress. In this report, we show that chronic inhalation exposure to $\text{PM}_{2.5}$ (10 months exposure) induces macrophage infiltration and Unfolded Protein Response (UPR), an intracellular stress signaling that regulates cell metabolism and survival, in mouse white adipose tissue *in vivo*. Gene expression studies suggested that $\text{PM}_{2.5}$ exposure induces two distinct UPR signaling pathways mediated through the UPR transducer inositol-requiring 1α (IRE1 α): 1) ER-associated Degradation (ERAD) of unfolded or misfolded proteins, and 2) Regulated IRE1-dependent Decay (RIDD) of mRNAs. Along with the induction of the UPR pathways and macrophage infiltration, expression of genes involved in lipogenesis, adipocyte differentiation, and lipid droplet formation was increased in the adipose tissue of the mice exposed to $\text{PM}_{2.5}$. *In vitro* study confirmed that $\text{PM}_{2.5}$ can trigger phosphorylation of the UPR transducer IRE1 α and activation of macrophages. These results provide novel insights into $\text{PM}_{2.5}$ -triggered cell stress response in adipose tissue and increase our understanding of pathophysiological effects of particulate air pollution on the development of metabolic disorders.

Keywords: Ambient particulate matter, $\text{PM}_{2.5}$, unfolded protein response, lipid metabolism, white adipose tissue

Introduction

Air pollution is a continuing world-wide challenge to public health. Epidemiologic and experimental investigations have consistently demonstrated a link between fine particulate matter (aerodynamic diameter $<2.5 \mu\text{m}$, $\text{PM}_{2.5}$) and susceptibility to cardiovascular disease [1]. The mechanisms by which $\text{PM}_{2.5}$ predisposes to cardiovascular events are *via* $\text{PM}_{2.5}$ interaction with pro-inflammatory pathways, hyper-coagulability, alterations in autonomic tone, and vasomotor alterations [1]. Indeed, the pathways mediating the effects of air pollution are indistinguishable from those triggered by other classic risk factors for cardiovascular disease

[1]. We have recently demonstrated that $\text{PM}_{2.5}$ exposure mediates early alterations in insulin resistance, visceral inflammation, and structural and functional alterations in brown adipose tissue [2-4]. We have also shown that $\text{PM}_{2.5}$ exposure induces endoplasmic reticulum (ER) stress and Unfolded Protein Response (UPR) characterized by activation of double-strand RNA-activated protein kinase-like ER kinase (PERK), leading to phosphorylation of translation initiation factor eIF2 α and induction of C/EBP homologous transcription factor CHOP/GADD153 in liver tissue [5]. $\text{PM}_{2.5}$ exposure stimulates inflammatory responses, disrupts insulin signaling, and represses peroxisome proliferator-activated receptor α (PPAR α) and

PM_{2.5} induces unfolded protein response

PPAR γ in the liver, leading to hepatic glycogen depletion, insulin resistance, and steatohepatitis [6]. Taken together, it has been shown the pathophysiologic effects of PM_{2.5} may occur *via* activation of intracellular stress responses and innate immune pathways and synergize with other triggers or risk factors, such as high-fat diet, leading to modulation of cell metabolism or death programs [2, 4, 7].

In eukaryotic cells, the ER is primary recognized as a compartment for protein folding and assembly [8]. A variety of biochemical, physiological, or pathological conditions can directly or indirectly interrupt the protein folding process, causing the accumulation of unfolded or misfolded proteins in the ER lumen—a condition referred to as “ER stress”. The UPR pathways are activated to help the cell adapt to ER stress conditions by remodeling transcriptional and translational programs. The basic UPR pathways are mediated through three primary ER-localized protein stress sensors: PERK (double-strand RNA-activated protein kinase-like ER kinase), IRE1 α (inositol-requiring 1 α), and ATF6 (activating transcription factor 6). The UPR signaling is known to intersect with a variety of inflammatory pathways as well as oxidative stress responses, all of which may influence lipid and glucose metabolism [9-12]. In this study, we demonstrated that long-term exposure to environmentally relevant PM_{2.5} induces macrophage infiltration and activation of distinct UPR pathways mediated through IRE1 α , including ER-associated Degradation (ERAD) and Regulated IRE1-dependent mRNA Decay (RIDD) [13], in mouse white adipose tissue. Along with activation of the UPR pathways and infiltration of macrophages, expression of the genes involved in lipogenesis, adipocyte differentiation, and lipid droplet formation was significantly increased in the adipose tissue of the mice exposed to PM_{2.5}. These results provide important mechanistic evidence that PM_{2.5} modulates inflammatory stress responses and lipid metabolism in fat tissue, which may partially explain the link between air pollution and development of metabolic syndrome.

Material and methods

Ethics statement

All animal works have been conducted according to relevant national and international guide-

lines. All the experimental procedures were performed in accordance with the recommendations of the Weatherall report, “The use of non-human primates in research”. The Committees on Use and Care of Animals at Ohio State University and Wayne State University approved all experimental procedures.

Animal model and ambient PM_{2.5} exposure

C57BL/6 male mice at six-weeks of age were purchased from the Jackson Laboratories (Bar Harbor, ME) and were housed in cages with regular chow in an Association for Assessment and Accreditation of Laboratory Animal Care-accredited animal housing facility. The Committees on Use and Care of Animals at the Ohio State University approved all experimental procedures. Mice were randomly assigned a group and were exposed to concentrated ambient PM_{2.5} or filtered air (FA) for 6 hours/day, 5 days/week from April 2009 to January 2010 in an exposure facility “Ohio’s Air Pollution Exposure System for the Interrogation of Systemic Effects” (OASIS)-1 in Columbus, OH, USA, as previously described [3]. The PM_{2.5} components to which the animals were exposed are primarily attributed to long-range transport [3]. The control mice in the experiment were exposed to an identical protocol with the exception of a high-efficiency particulate-air filter positioned in the inlet valve position to remove all of the PM_{2.5} in the filtered air (FA) stream. On the final day of the exposure, the mice were euthanized and tissue samples were collected for further studies.

Energy-dispersive x-ray fluorescence (ED-XRF)

All particle samples for gravimetric and elemental analyses were collected on filters. Filter masses were measured on a microbalance (model MT5, Mettler-Toledo Inc., Highstown, NJ). Analyses for major elements followed by nondestructive XRF (model EX-6600-AF, Jordan Valley) using five secondary fluorescers (Si, Ti, Fe, Ge, and Mo) and spectral software XRF2000v3.1 (U.S. EPA and ManTech Environmental Technology, Inc.) as described elsewhere [14].

In vitro exposure to PM_{2.5}

For PM_{2.5} *in vitro* exposure experiments, the Teflon filters used for gravimetric and elemen-

PM_{2.5} induces unfolded protein response

tal analyses were placed downstream of the cyclone inlet of the "OASIS-1" exposure system to collect ambient particulates as previously described [14-16]. PM_{2.5} was collected during mouse exposure. Mouse monocyte/macrophage cell line RAW264.7 was treated with PM_{2.5} at the concentration of 5 µg/ml, and the same volume of PBS was added in the control group.

Hematoxylin and eosin (H&E), immunohistochemistry or immunofluorescence staining

H&E staining was performed on paraffin-embedded tissue sections (5 µm) of mouse epididymal adipose tissue. Sections were placed on slides, deparaffinized in xylene, hydrated in graded ethanol, and rinsed in distilled water as previously described [11]. Slides were incubated in Harris Hematoxylin (Sigma) for 3 minutes and dipped in Scott's Tap Water (Sigma) 5 times. Sections were counterstained in eosin (Sigma) for 10 minutes. Slides were dehydrated in 100% ethanol and cleared in xylene. Permount (Fisher) was used to mount slides. For immunohistochemistry staining, the 5 µm adipose tissue sections were blocked with 0.5% H₂O₂ in methanol to reduce endogenous peroxidase activity. The sections were incubated with anti-BiP/GRP78 antibody (1:100) overnight at 4°C. The slide sections were washed and then incubated with the second antibody conjugated with HRP at room temperature for 2 hours. Sections were developed in VECTASTAIN peroxidase substrate (Vector laboratories, Burlingame, California) and counterstained with hematoxylin. Immunofluorescent staining of mouse monocyte/macrophage cell line RAW264.7 was performed based on the standard protocol. Briefly, RAW264.7 cells cultured on glass cover-slips were fixed with ice-cold methanol for 20 minutes, blocked with 1% BSA in PBS, and then incubated with anti-F4/80 (1:200) antibody in blocking solution overnight at 4°C. The nucleus was stained with DAPI. The cells were then incubated with Alexa fluor 488 (Invitrogen) for 1 hour at room temperature before being mounted and examined by fluorescent microscopy.

Quantitative real-time reverse-transcription (RT-PCR)

Epididymal mouse adipose tissues from the mice were excised, and RNA was isolated using

Trizol reagent according to the manufacturer's instructions. The cDNAs were synthesized from mRNA templates using SuperScript III First-Strand Synthesis SuperMix for qRT-PCR (Invitrogen). Real-time PCR was performed using a reaction mix of cDNA, primers, and Fast SYBR Green Master Mix (Applied Bioscience). Samples were denatured at 95°C for 20 seconds then cycled between 95°C (3 seconds) and 60°C (30 seconds) using the 7500 Fast Real-Time PCR System (Applied Biosystems). The sequences of primers for examining the regulated IRE1-dependent decay (RIDD) were previously as previously described [13]. The other real-time PCR primer sequence information is shown in [Supplemental Information](#). Fold changes of mRNA levels were determined after normalization to internal control β-actin RNA levels.

Western blot analysis

Total cell lysates were prepared from cultured RAW264.7 cells using NP-40 lysis buffer (1% NP-40, 50 mM Tris-HCl, pH 7.5, 150 mM NaCl, 0.05% SDS, 0.5 mM Na vanadate, 100 mM NaF, 50 mM β-glycerophosphate, and 1 mM phenylmethylsulfonyl fluoride) supplemented with protease inhibitors (EDTA-free Complete Mini, Roche). Denatured proteins were separated by SDS-PAGE on 10% Tris-glycine polyacrylamide gels and transferred to a 0.45-mm PVDF membrane (GE Healthcare). The membrane was incubated with a rabbit polyclonal anti-phosphorylated IRE1α antibody (Abcam, 1:1000), or rabbit polyclonal anti-IRE1α antibody (Cell Signaling Technologies, 1:1000) as the primary antibody, and a HRP-conjugated anti-rabbit secondary antibody. Membrane-bound antibodies were detected by an enhanced chemiluminescence detection reagent (GE Healthcare). Levels of α-tubulin were determined as loading controls. The signal intensities were determined by Quantity One 4.6.7 (Bio-Rad Life Science, CA). The ratios of signal intensities of phosphorylated IRE1α to that of total IRE1α were first determined. The fold changes of IRE1α phosphorylation in PM_{2.5}-exposed RAW264.7 cells were determined by comparing IRE1α phosphorylation ratio in PM_{2.5}-exposed RAW264.7 cells to that in vehicle-exposed control RAW264.7 cells (100%). All *in vitro* experiments were repeated at least three times independently.

PM_{2.5} induces unfolded protein response

Statistics

Experimental results are shown as mean \pm SEM (for variation between animals or experiments). The mean values for biochemical data from the experimental groups (PM_{2.5} exposure versus filtered air) were compared by a paired or unpaired, 2-tailed Student's *t* test. Statistical tests with $P < 0.05$ were considered significant.

Results

PM_{2.5} exposure leads to macrophage infiltration in white adipose tissue

To elucidate *in vivo* effect of long-term PM_{2.5} exposure, male C57BL/6J mice were exposed to concentrated ambient PM_{2.5} for 10 months in the "OASIS-1" exposure system composed of the Midwestern regional background in Columbus, OH, where most of the PM_{2.5} is attributed to long-range transport [5, 17, 18]. The "OASIS-1" is a versatile aerosol concentration enrichment system through which PM_{2.5} fine and ultrafine particles are concentrated and exposed to the animals in the chamber [19, 20]. It has been demonstrated that the distribution and size of concentrated PM_{2.5} collected from the exposure chamber air truly reflect that of non-concentrated PM_{2.5} present in the ambient air [19-21]. The mobile OASIS-1 system allows us to perform the studies on animal models that recapitulate true personal, long-term exposure to environmental relevant PM_{2.5}. During the exposure time period, the mean daily PM_{2.5} concentration was 12.7 (s.d., 8.4) $\mu\text{g}/\text{m}^3$. The mean concentration of PM_{2.5} in the exposure chamber was 94.4 $\mu\text{g}/\text{m}^3$ (~ 7-fold of ambient PM_{2.5} levels). The control mice in the experiment were exposed to an identical protocol with the exception of a high-efficiency particulate-air filter positioned in the inlet valve position to remove all of the PM_{2.5} in the filtered air stream. The X-ray fluorescence spectroscopic analysis of PM_{2.5} composition in the exposure chamber revealed higher concentration of a range of metals [18]. During the exposure, the major composition of PM_{2.5} included alkali metals (K and Na), alkaline earth metals (Mg and Ca), transition metals (Fe and Zn), and non-metals (S) (Table 1).

Our previous studies demonstrated that long-term ambient PM_{2.5} exposure induces inflammation and mitochondrial alteration in mouse adipose tissues [3, 22]. White adipose tissue

(WAT) has been recognized as an endocrine and secretory organ that plays key roles in the development of metabolic syndrome. To further delineate the impact of PM_{2.5} exposure on WAT, we first examined whether long-term PM_{2.5} exposure causes morphological changes in mouse WAT. H&E staining revealed increased cell infiltration in the WAT of the mice exposed to PM_{2.5}, compared to that in the mice exposed to FA (Figure 1A). Based on the morphology of infiltrated tissue, the invading cells in WAT upon PM_{2.5} exposure are likely macrophages. To further characterize this observation, we stained the mouse WAT for mature macrophage cell surface F4/80. The F4/80 staining result confirmed activated macrophages invading the WAT of the PM_{2.5}-exposed mice (Figure 1B).

PM_{2.5} exposure induces ER stress in white adipose tissue

In addition to macrophage infiltration, we also observed enlargement of adipocytes in WAT of the PM_{2.5}-exposed mice. H&E staining indicated that sizes of adipocytes in WAT of the mice after 10-months PM_{2.5} exposure were significantly enlarged, compared to those in the mice after FA exposure (Figure 2A). The expansion of adipocytes may be partially due to inflammation and oxidative stress in fat tissue upon PM_{2.5} exposure, as we previously addressed [3]. To gain further understanding of the molecular basis responsible for the phenotype observed in the WAT of the PM_{2.5}-exposed animals, we asked whether inhalation exposure to PM_{2.5} (whole-body PM_{2.5} exposure) can trigger ER stress response, a fundamental intracellular stress signaling that has profound impact in cell pathophysiology, in mouse WAT. We examined induction of the ER chaperone protein GRP78/BiP, a hall marker of ER stress and the master regulator of the UPR signaling, in the WAT of the PM_{2.5}-exposed mice. Immunohistochemical staining showed that induction of BiP was increased in the WAT of the PM_{2.5}-exposed animals, compared to that in the FA-exposed animals (Figure 2B), suggesting activation of ER stress response in the WAT upon PM_{2.5} exposure.

PM_{2.5} exposure activates ERAD- and RIDD- UPR pathways in white adipose tissue

To delineate the UPR pathways in WAT triggered by PM_{2.5} exposure, we performed quantitative

PM_{2.5} induces unfolded protein response

Table 1. Elemental concentrations of PM_{2.5} particle during the exposure period from April 2009 to January 2010*

Element	Mean (ng/m ³)	Minimum (ng/m ³)	Maximum (ng/m ³)
S	6910.81	40.96	16786.91
Si	1010.19	211.04	2637.09
Ca	555.27	6.16	1411.00
Fe	512.54	6.87	1675.01
Na	380.35	46.97	1770.28
Al	341.13	83.42	790.83
K	224.45	56.99	620.01
Mg	171.84	21.46	333.92
P	170.01	13.59	509.56
Zn	86.52	10.07	295.51
Cl	47.80	0.14	188.52
Mn	25.94	3.18	102.46
Pb	17.89	3.40	43.18
Ti	17.53	3.21	69.72
Cd	16.42	4.05	38.68
Br	15.97	0.03	65.45
Cu	14.09	1.75	47.15
Cs	10.88	2.12	38.40
Se	10.20	1.53	40.56
Co	8.77	0.43	30.79
Sc	6.49	0.06	18.85
As	6.19	0.79	27.20
Cr	4.50	0.25	11.42
I	3.82	3.83	75.79
Sr	3.81	0.05	13.48
Ni	2.26	0.25	7.76
Ga	1.87	0.08	13.55
Rb	0.52	0.001	4.83

*All PM_{2.5} samples for gravimetric and elemental analyses were collected on filters. Analyses for major elements followed by nondestructive Energy-Dispersive X-Ray Fluorescence using five secondary fluorescers and spectral software XRF2000v3.1.

real-time RT-PCR analysis of gene expression involved in ER stress and UPR signaling in WAT from the mice exposed to PM_{2.5} or FA. Levels of spliced *Xbp1* mRNA, a target of ER stress sensor IRE1 α RNase activity and a potent trans-activator of ERAD [8], were increased in the WAT of the mice exposed to PM_{2.5} (**Figure 3A**). Expression levels of the mRNAs encoding key components in ERAD including ER degradation enhancer, mannosidase alpha-like 1 (*Edem1*) and Der1-like domain family member 1 (*Der11*), which are regulated by the UPR pathway through IRE1 α /XBP1, were also increased in the WAT of PM_{2.5}-exposed mice (**Figure 3A**). EDEM1 is known to extract misfolded glycopro-

teins from the calnexin cycle for their degradation in an N-glycan-independent manner [23, 24]. DERL1 acts in the ERAD pathway by forming a channel that allows the retrotranslocation of misfolded proteins into the cytosol where they are ubiquitinated and degraded by the proteasome. Up-regulation of spliced *Xbp1*, *Edem1*, and *Der11* mRNAs in PM_{2.5}-exposed mouse WAT suggests a distinct effect of PM_{2.5} exposure on accumulation of misfolded proteins in the ER and activation of IRE1 α /XBP1-regulated ERAD pathway in WAT.

PM_{2.5} exposure also induces RIDD, a pathway mediated by the UPR transducer IRE1 α to promote rapid turnover of mRNAs encoding membrane and secreted proteins [13]. Quantitative real-time RT-PCR analysis demonstrated that levels of the RIDD targets, including the *Pmp22*, *Col6*, *HgNat*, *Blos1*, *Scara3*, and *Pdgfr* mRNAs [13], were all decreased in the WAT of mice exposed to PM_{2.5} (**Figure 3B**), indicating the activation of RIDD pathway upon PM_{2.5} exposure.

PM_{2.5} exposure stimulates lipogenesis, lipid deposition, and adipocyte differentiation

It has been demonstrated that enhanced lipogenesis and lipid droplet formation is associated with ER stress response in the liver or adipose tissues [12, 25-27]. To determine whether PM_{2.5} exposure affects lipid metabolism in WAT, we examined expression levels of genes regulating lipogenesis, lipid transport, and lipid droplet formation in WAT of PM_{2.5} or FA-exposed mice. A significant increase of the lipogenic gene acetyl-CoA carboxylase (*Acaca*) was observed in PM mice (**Figure 3C**). ACACA facilitates the conversion of acetyl-CoA to malonyl-CoA, the rate limiting step of fatty acid synthesis [28]. Expression of the long-chain fatty acid transporter, *Fat/Cd36*, was also significantly increased in WAT of PM_{2.5}-exposed mice (**Figure 3C**), indicating an increase in fatty acid uptake and deposition [29]. Additionally, expression of the key enzyme that catalyzes TG synthesis, diglyceride acyltransferase 2

PM_{2.5} induces unfolded protein response

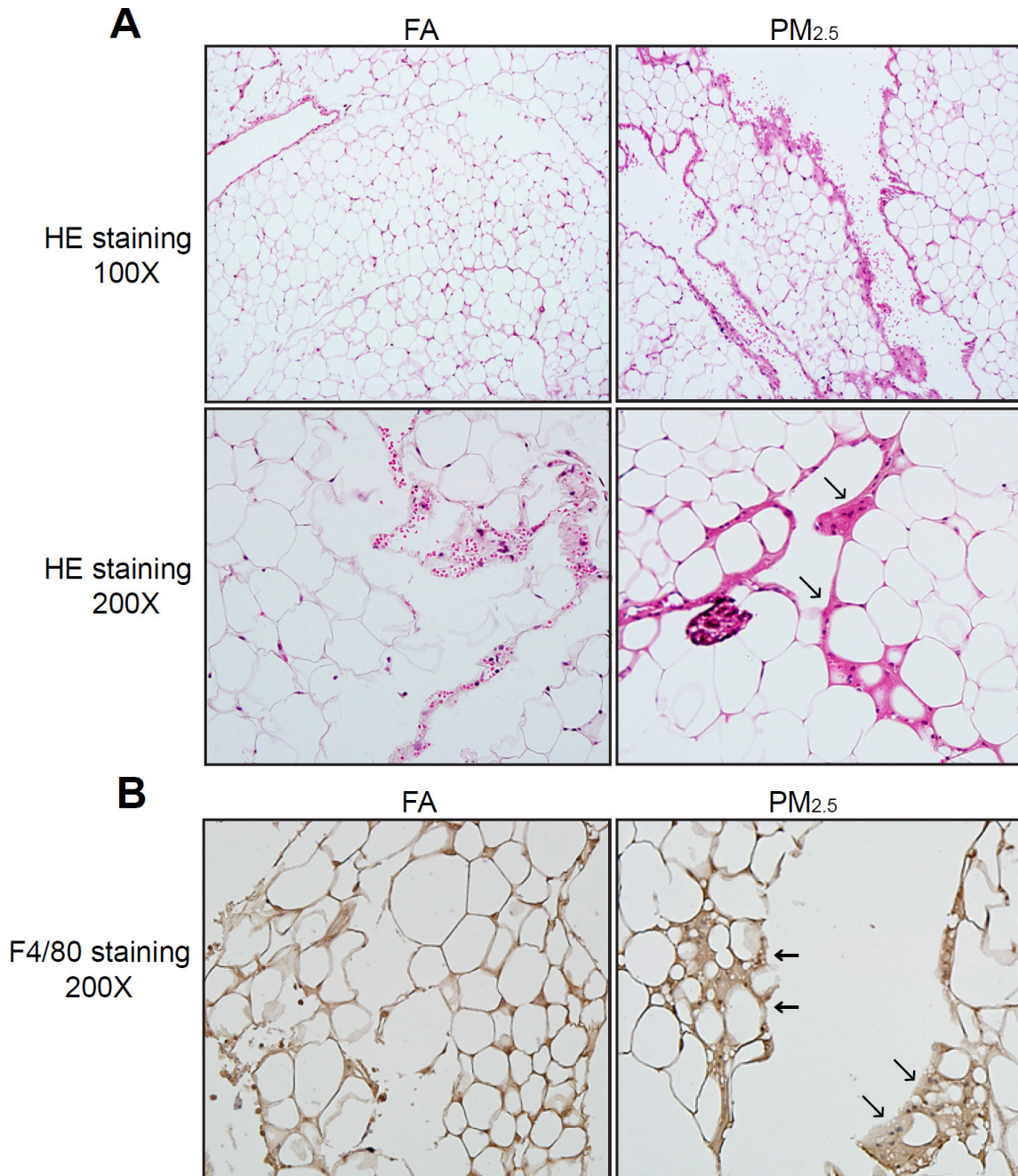


Figure 1. Inhalation exposure to PM_{2.5} leads to macrophage infiltration and activation in WAT. A: H&E staining of WAT sections from mice after PM_{2.5} or FA exposure for 10 months. Magnifications: 100× (upper panel) and 200× (lower panel). The arrows point out the macrophage-infiltrated areas. B: F4/80 staining of WAT sections from mice after PM_{2.5} or FA exposure for 10 months. Magnification: 200×. The arrows point out the macrophage-infiltrated, F4/80-positive areas. For A-B, staining of adipose tissue sections from 4 mice was performed and representative staining results were shown.

(*Dgat2*), and hormone sensitive lipase (*Lipe*), which catalyzes the rate-limiting step of triglyceride breakdown, was increased in WAT upon PM_{2.5} exposure (Figure 3C). These increases may represent an adaptive response in adipose

tissue to increased levels of triglycerides [30, 31].

White adipocytes contain a large single lipid droplet surrounded by a layer of cytoplasm.

PM_{2.5} induces unfolded protein response

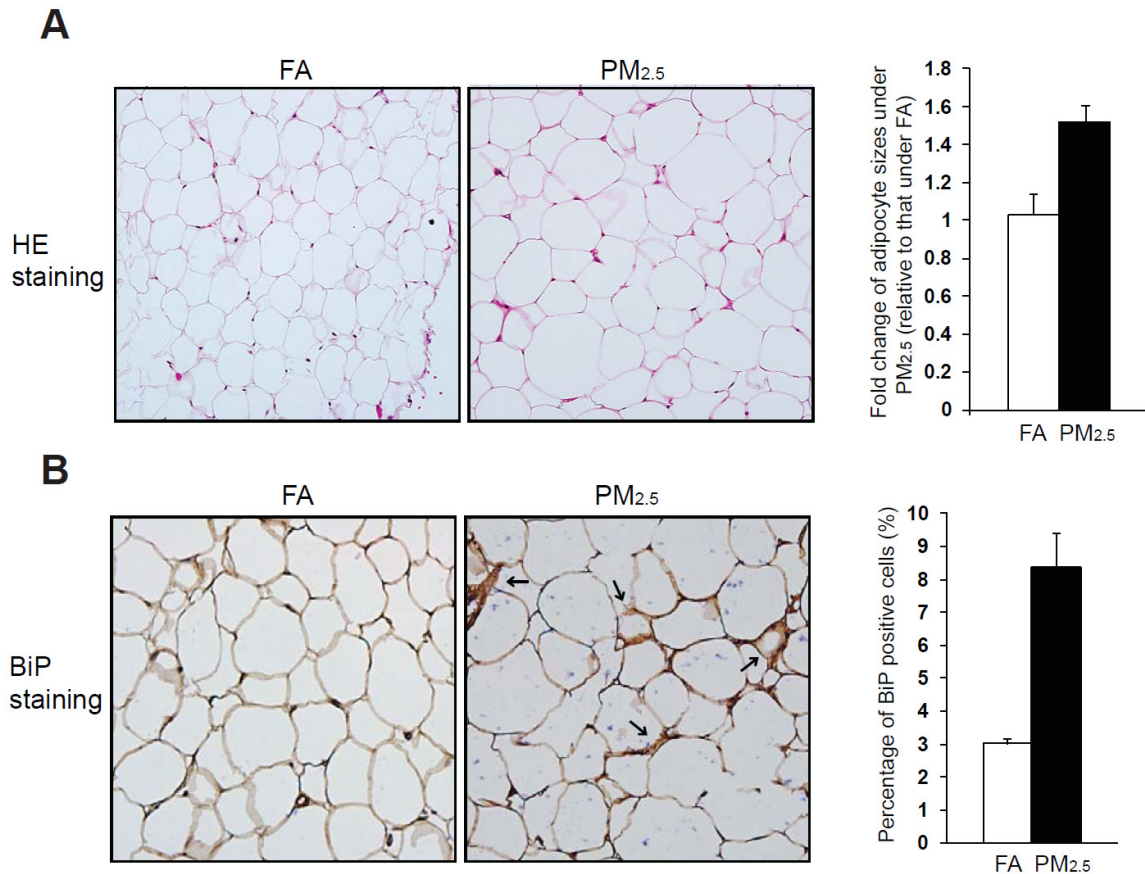


Figure 2. Exposure to PM_{2.5} enlarges adipocytes and induces BiP expression in mouse WAT. **A:** H&E staining of WAT sections from mice after PM_{2.5} or FA exposure for 10 months. Magnification: 200×. The graph beside the image shows fold change of adipocyte sizes under PM_{2.5} exposure relative to those under FA. For the tissue section from each animal, sizes of adipocytes from 3 representative tissue areas per mouse were calculated to obtain the average adipocyte size. Each bar denotes the mean ± SEM (n=4 mice/group). **B:** BiP/GRP78 staining of WAT sections from mice after PM_{2.5} or FA exposure for 10 months. Magnification: 200×. The graph beside the image shows percentages of BiP staining-positive adipocytes to total adipocytes in mice under PM_{2.5} or FA exposure. The arrows point out the positive staining. For the tissue section from each animal, percentages of BiP staining-positive adipocytes from 3 representative tissue areas per mouse were calculated to obtain the average value. Each bar denotes the mean ± SEM (n=3 mice for the FA exposure group and 2 mice for PM_{2.5} exposure group).

Consistent with enlarged cell sizes and increased lipogenesis in WAT upon PM_{2.5} exposure, expression of genes encoding functions in adipocyte differentiation and lipid droplet formation, including small adipocyte factor 1 (*Smaf1*), Carcinoembryonic antigen-related cell adhesion molecule 1 (*Ceacam1*), adipocyte-specific protein fat-specific protein 27 (*Fsp27*), Perilipin 1 (*Plin1*), and fat-inducing transcript 2 (*Fit2*), was increased in mouse WAT upon PM_{2.5} exposure (**Figure 3D**). Additionally, induction of Adipsin, an adipokine that plays important roles in autoimmunity, glucose transport, and triglyceride accumulation in fat tissues [32], was also increased in WAT of the PM_{2.5}-exposed mice

(**Figure 3E**). Taken together, these results indicate the stress responses triggered by PM_{2.5} facilitate de novo lipogenesis, lipid accumulation, and adipocyte differentiation. This is consistent with the enlarged adipocytes observed in mouse WAT upon PM_{2.5} exposure (**Figure 2A**).

PM_{2.5} exposure activates macrophages and the UPR transducer IRE1α in vitro

Our previous studies demonstrated that circulating or resident macrophages are primary targets of whole-body PM_{2.5} exposure in mediating inflammatory stress responses [5, 6]. As our

PM_{2.5} induces unfolded protein response

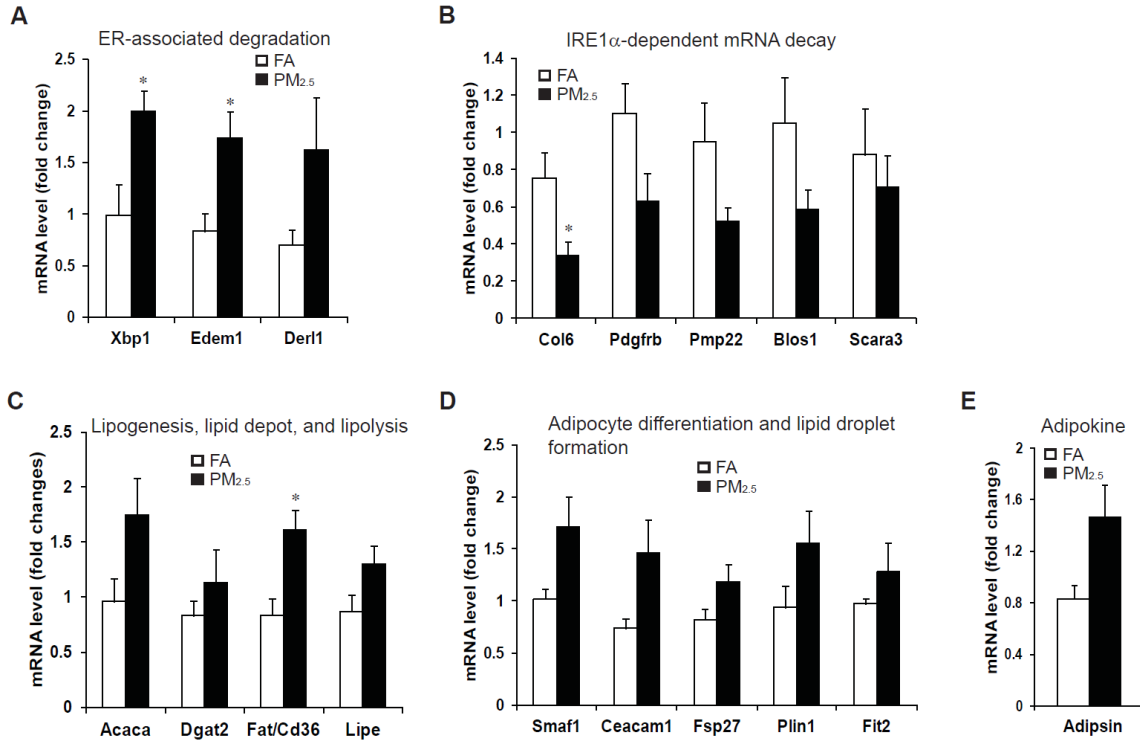


Figure 3. Exposure to PM_{2.5} induces expression of genes involved in UPR pathways and lipid metabolism in mouse WAT. Quantitative real-time PCR analysis of expression of genes involved in ER-associated degradation (A), IRE1 α -dependent mRNA decay (B), lipogenesis, lipid deposition, and lipolysis (C), adipocyte differentiation and lipid droplet formation (D), and adipin (E) in WAT of mice after PM_{2.5} or FA exposure for 10 months. Fold changes of mRNA levels were determined after normalization to internal control β -actin RNA levels. For each comparison group, the mRNA level of one FA-exposed mouse was defined as 1, and was used to calculate the fold changes of mRNA levels for the other mice. Each bar denotes the mean \pm SEM (n = 4 mice/group), *p < 0.05.

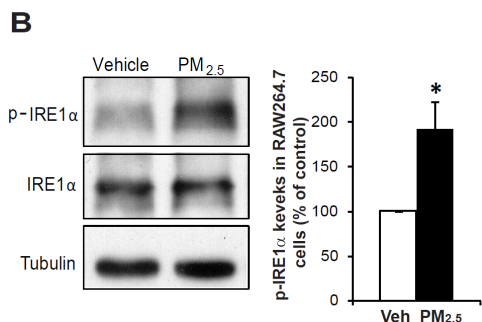
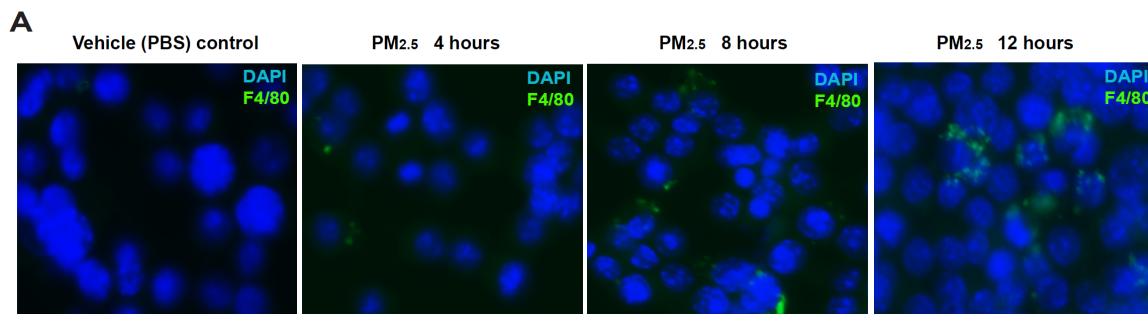


Figure 4. PM_{2.5} exposure activates macrophages and the UPR transducer IRE1 α *in vitro*. A: Immunofluorescent analysis of F4/80 induction in RAW264.7 cells cultured in the presence of vehicle (PBS) or 5 μ g/ml PM_{2.5} particles for 4, 8, and 12 hours, respectively. The cells were stained for F4/80 (green) and counterstained with DAPI for nucleus (blue). The experiment was repeated 3 times, and representative data was shown. Magnification: 400 \times . B: Western blot analysis of levels of phosphorylated and total IRE1 α in RAW264.7 cells exposed to PM_{2.5} or vehicle (PBS) for 12 hours. Levels of tubulin were determined as loading controls. The experiment was repeated 3 times, and representative data was shown. The graph beside the images showed percentages of phosphorylated IRE1 α (compared to total IRE1 α) in the PM_{2.5}- or vehicle-exposed RAW264.7 cells. Each bar denotes the mean \pm SEM (n = 3 biological replications). * p < 0.05; Veh, vehicle.

PM_{2.5} induces unfolded protein response

animal experiments have shown that PM_{2.5} exposure stimulates macrophage infiltration and activation in WAT (**Figure 1**), we tested whether PM_{2.5} can activate macrophages *in vitro*. Cultured mouse monocyte/macrophage cell line RAW264.7 was exposed to 5µg/ml of PM_{2.5} for 4, 8, and 12 hours, respectively. Activation of macrophages, as evidenced by F4/80 staining, was increased upon PM_{2.5} exposure in a time-dependent manner (**Figure 4A**). Next, we tested whether PM_{2.5} can induce UPR signaling in macrophages *in vitro*. Upon 12 hours of PM_{2.5} exposure, levels of phosphorylated IRE1α, an indicator of the IRE1α-mediated UPR signaling, were significantly increased in RAW264.7 cells (**Figure 4B**). This result supports the effect of PM_{2.5} on activation of the UPR signaling pathways mediated through IRE1α in the macrophage-infiltrated WAT from PM_{2.5}-exposed animals (**Figure 3A** and **3B**).

Discussion

Traffic-related airborne PM_{2.5} is a complex mixture of particles and gases from gasoline and diesel engines, together with dust from wear of road surfaces, tires, and brakes [33, 34]. Airborne PM_{2.5} demonstrates an incremental capacity to penetrate into the distal airway units and potentially enter the systemic circulation with diminishing sizes. Recent studies suggested that traffic-related PM may promote cardiovascular and/or metabolic diseases [17, 35, 36]. Disruption of adipose endocrine and metabolic function is thought to play a key role in dysregulated lipid and energy homeostasis, which is characteristic of disorders, such as obesity and type II diabetes. Recently, our group has reported the effects of chronic air-pollution exposure on the development of metabolic dysfunction. We have provided evidence that exposure to PM_{2.5} leads to visceral adipose inflammation and oxidative stress along with alterations in levels of circulating adipokines, including adiponectin and leptin [3, 22]. PM_{2.5} exposure also significantly reduces mitochondria in both WAT and brown adipose tissue (BAT) and induces ER stress response in the liver [5]. Inhalation exposure to PM_{2.5} stimulates hepatic inflammation, depletes glycogen storage, and promotes lipid accumulation in the liver, contributing to glucose intolerance and insulin resistance [6]. The pathophysiological effects of PM_{2.5} exposure on

the liver apparently account for the development of metabolic syndrome under air pollution. In this study, we delineated the nature of the inflammatory stress response and alteration in lipid metabolic pathways in visceral adipose tissue triggered by PM_{2.5} exposure. Our study suggests that PM_{2.5} exposure in WAT induces ER stress and activates ERAD and RIDD, two unique UPR signaling pathways mediated through the UPR transducer IRE1α (**Figures 3** and **4**). Along with ER stress response, expression of the genes involved in lipogenesis, lipolysis, adipocyte differentiation, and lipid droplet formation was increased in WAT of the mice exposed to PM_{2.5} (**Figure 3**). These findings represent important new insights into the effects of PM_{2.5} exposure on metabolic disorders, such as type-II diabetes and obesity.

Based on our previous and current studies, inflammation, oxidative stress, and ER stress response are likely integrated in the liver and adipose tissue where they may form a “stress loop” that contributes to alteration in lipid and energy metabolism under PM_{2.5} exposure [3, 6, 9, 22, 37]. During this process, macrophage is the key player in mediating inflammatory stress responses in both liver and fat tissues under air pollutant exposure. Presumably, infiltrated macrophages, as we observed in WAT under PM_{2.5} exposure (**Figure 1**), may be primarily responsible for inflammation and ER stress response in WAT triggered by PM_{2.5}. This interesting scenario needs to be further elucidated in the future.

Under ER stress, splicing of *Xbp1* mRNA by the UPR transducer IRE1α is a prerequisite for production of the functional UPR *trans*-activator XBP1 [9]. We previously showed that PM_{2.5} exposure can activate IRE1α, but suppresses splicing of *Xbp1* mRNA in liver tissues [5]. However, the current study showed that PM_{2.5} exposure can induce both IRE1α activation and *Xbp1* mRNA splicing in WAT (**Figures 3** and **4**). This discrepancy in *Xbp1* mRNA splicing under PM_{2.5} exposure may be due to the differences in target tissues/cell types as well as PM_{2.5} exposure times and concentrations. PM_{2.5} exposure activates IRE1α in WAT, which mediates both *Xbp1* mRNA splicing and RIDD pathway (**Figures 3** and **4**). In contrast, PM_{2.5} only activates IRE1α-mediated RIDD, but not *Xbp1* mRNA splicing, in

the liver tissue [5]. It is interesting to elucidate the conditions under which PM_{2.5} induces or suppresses *Xbp1* mRNA splicing and its related pathophysiologic impact in the future. Moreover, for future research, whether alterations in ER stress are a cause or consequence of PM_{2.5} exposure and the temporality of these changes are important subjects to pursue. Whether the response in WAT occurs congruently with hepatic ER stress response that we previously demonstrated [5], and whether hepatic ER stress is a pre-requisite for functional changes in the adipose tissue also deserve further investigation.

Acknowledgement

Portions of this work were supported by National Institutes of Health (NIH) grants DK090313 and ES017829 to KZ, and NIH ES018900 to QS. RM is supported by a training grant provided by NIGMS R25GM058905.

Address correspondence to: Dr. Kezhong Zhang, Center for Molecular Medicine and Genetics, Wayne State University School of Medicine, 540 E. Canfield Avenue, Detroit, MI 48201, USA. Phone: 313-577-2669; Fax: 313-577-5218; E-mail: kzhang@med.wayne.edu; Dr. Qinghua Sun, Division of Environmental Health Sciences, College of Public Health, Ohio State University, Columbus, OH 43210, USA. Phone: 614-247-1560; Fax: 614-688-4233; E-mail: sun.224@osu.edu

References

- [1] Brook RD, Rajagopalan S. Particulate matter air pollution and atherosclerosis. *Curr Atheroscler Rep* 2010; 12: 291-300.
- [2] Sun Q, Yue P, Deiluiis JA, Lumeng CN, Kampfrath T, Mikolaj MB, Cai Y, Ostrowski MC, Lu B, Parthasarathy S, Brook RD, Moffatt-Bruce SD, Chen LC, Rajagopalan S. Ambient Air Pollution Exaggerates Adipose Inflammation and Insulin Resistance in a Mouse Model of Diet-Induced Obesity. *Circulation* 2009; 119: 538-546.
- [3] Xu X, Liu C, Xu Z, Tzan K, Zhong M, Wang A, Lippmann M, Chen LC, Rajagopalan S, Sun Q. Long-term Exposure to Ambient Fine Particulate Pollution Induces Insulin Resistance and Mitochondrial Alteration in Adipose Tissue. *Toxicol Sci* 2011; 124: 88-98.
- [4] Xu X, Yavar Z, Verdin M, Ying Z, Mihai G, Kampfrath T, Wang A, Zhong M, Lippmann M, Chen LC, Rajagopalan S, Sun Q. Effect of early particulate air pollution exposure on obesity in mice: role of p47phox. *Arterioscler Thromb Vasc Biol* 2010; 30: 2518-2527.
- [5] Laing S, Wang G, Briazova T, Zhang C, Wang A, Zheng Z, Gow A, Chen AF, Rajagopalan S, Chen LC, Sun Q, Zhang K. Airborne particulate matter selectively activates endoplasmic reticulum stress response in the lung and liver tissues. *Am J Physiol Cell Physiol* 2010; 299: C736-749.
- [6] Zheng Z, Xu X, Zhang X, Wang A, Zhang C, Hüttemann M, Grossman LI, Chen LC, Rajagopalan S, Sun Q, Zhang K. Exposure to Ambient Particulate Matter Induces a NASH-like Phenotype and Impairs Hepatic Glucose Metabolism in an Animal Model. *J Hepatol* 2013 Jan; 58: 148-54.
- [7] Kampfrath T, Maiseyeu A, Ying Z, Shah Z, Deiluiis JA, Xu X, Kherada N, Brook RD, Reddy KM, Padture NP, Parthasarathy S, Chen LC, Moffatt-Bruce S, Sun Q, Morawietz H, Rajagopalan S. Chronic fine particulate matter exposure induces systemic vascular dysfunction via NADPH oxidase and TLR4 pathways. *Circ Res* 2011; 108: 716-726.
- [8] Ron D, Walter P. Signal integration in the endoplasmic reticulum unfolded protein response. *Nat Rev Mol Cell Biol* 2007; 8: 519-529.
- [9] Zhang K, Kaufman RJ. From endoplasmic-reticulum stress to the inflammatory response. *Nature* 2008; 454: 455-462.
- [10] Zhang C, Wang G, Zheng Z, Maddipati KR, Zhang X, Dyson G, Williams P, Duncan SA, Kaufman RJ, Zhang K. Endoplasmic reticulum-tethered transcription factor cAMP responsive element-binding protein, hepatocyte specific, regulates hepatic lipogenesis, fatty acid oxidation, and lipolysis upon metabolic stress in mice. *Hepatology* 2012; 55: 1070-1082.
- [11] Zheng Z, Zhang C, Zhang K. Measurement of ER stress response and inflammation in the mouse model of nonalcoholic fatty liver disease. *Methods Enzymol* 2011; 489: 329-348.
- [12] Zhang K, Wang S, Malhotra J, Hassler JR, Back SH, Wang G, Chang L, Xu W, Miao H, Leonardi R, Chen YE, Jackowski S, Kaufman RJ. The unfolded protein response transducer IRE1alpha prevents ER stress-induced hepatic steatosis. *EMBO J* 2011; 30: 1357-1375.
- [13] Hollien J, Lin JH, Li H, Stevens N, Walter P, Weissman JS. Regulated Ire1-dependent decay of messenger RNAs in mammalian cells. *J Cell Biol* 2009; 186: 323-331.
- [14] Maciejczyk P, Chen LC. Effects of subchronic exposures to concentrated ambient particles (CAPs) in mice. VIII. Source-related daily variations in in vitro responses to CAPs. *Inhal Toxicol* 2005; 17: 243-253.
- [15] Sun Q, Yue P, Ying Z, Cardounel AJ, Brook RD, Devlin R, Hwang JS, Zweier JL, Chen LC, Rajagopalan S. Air pollution exposure potentiates hypertension through reactive oxygen species-

PM_{2.5} induces unfolded protein response

- mediated activation of Rho/ROCK. *Arterioscler Thromb Vasc Biol* 2008; 28: 1760-1766.
- [16] Sun Q, Yue P, Kirk RI, Wang A, Moatti D, Jin X, Lu B, Schecter AD, Lippmann M, Gordon T, Chen LC, Rajagopalan S. Ambient air particulate matter exposure and tissue factor expression in atherosclerosis. *Inhal Toxicol* 2008; 20: 127-137.
- [17] Sun Q, Wang A, Jin X, Natanzon A, Duquaine D, Brook RD, Aguinaldo JG, Fayad ZA, Fuster V, Lippmann M, Chen LC, Rajagopalan S. Long-term air pollution exposure and acceleration of atherosclerosis and vascular inflammation in an animal model. *JAMA* 2005; 294: 3003-3010.
- [18] Ying Z, Yue P, Xu X, Zhong M, Sun Q, Mikolaj M, Wang A, Brook RD, Chen LC, Rajagopalan S. Air pollution and cardiac remodeling: a role for RhoA/Rho-kinase. *Am J Physiol Heart Circ Physiol* 2009; 296: H1540-1550.
- [19] Maciejczyk P, Zhong M, Li Q, Xiong J, Nadziejko C, Chen LC. Effects of subchronic exposures to concentrated ambient particles (CAPs) in mice. II. The design of a CAPs exposure system for biometric telemetry monitoring. *Inhal Toxicol* 2005; 17: 189-197.
- [20] Su Y, Sipin MF, Spencer MT, Qin X, Moffet RC, Shields LG, Prather KA, Venkatachari P, Jeong C, Kim E, Hopke PK, Gelein RM, Utell MJ, Oberdorster G, Berntsen J, Devlin RB, Chen LC. Real-Time Characterization of the Composition of Individual Particles Emitted From Ultrafine Particle Concentrators. *Aerosol Science and Technology* 2006; 40: 19.
- [21] Chen LC, Nadziejko C. Effects of subchronic exposures to concentrated ambient particles (CAPs) in mice. V. CAPs exacerbate aortic plaque development in hyperlipidemic mice. *Inhal Toxicol* 2005; 17: 217-224.
- [22] Xu Z, Xu X, Zhong M, Hotchkiss IP, Lewandowski RP, Wagner JG, Bramble LA, Yang Y, Wang A, Harkema JR, Lippmann M, Rajagopalan S, Chen LC, Sun Q. Ambient particulate air pollution induces oxidative stress and alterations of mitochondria and gene expression in brown and white adipose tissues. *Part Fibre Toxicol* 2011; 8: 20.
- [23] Molinari M, Calanca V, Galli C, Lucca P, Paganetti P. Role of EDEM in the release of misfolded glycoproteins from the calnexin cycle. *Science* 2003; 299: 1397-1400.
- [24] Oda Y, Hosokawa N, Wada I, Nagata K. EDEM as an acceptor of terminally misfolded glycoproteins released from calnexin. *Science* 2003; 299: 1394-1397.
- [25] Lee JS, Mendez R, Heng HH, Yang ZQ, Zhang K. Pharmacological ER stress promotes hepatic lipogenesis and lipid droplet formation. *Am J Transl Res* 2012; 4: 102-113.
- [26] Lee JS, Zheng Z, Mendez R, Ha SW, Xie Y, Zhang K. Pharmacologic ER stress induces non-alcoholic steatohepatitis in an animal model. *Toxicol Lett* 2012; 211: 29-38.
- [27] Sha H, He Y, Chen H, Wang C, Zenno A, Shi H, Yang X, Zhang X, Qi L. The IRE1alpha-XBP1 pathway of the unfolded protein response is required for adipogenesis. *Cell Metab* 2009; 9: 556-564.
- [28] Schneider R, Guerra CE, Lampl M, Tatzert V, Zellnig G, Klein HL, Kohlwein SD. A novel cold-sensitive allele of the rate-limiting enzyme of fatty acid synthesis, acetyl coenzyme A carboxylase, affects the morphology of the yeast vacuole through acylation of Vac8p. *Mol Cell Biol* 2000; 20: 2984-2995.
- [29] Ibrahim A, Abumrad NA. Role of CD36 in membrane transport of long-chain fatty acids. *Curr Opin Clin Nutr Metab Care* 2002; 5: 139-145.
- [30] Liu Y, Xue C, Zhang Y, Xu Q, Yu X, Zhang X, Wang J, Zhang R, Gong X, Guo C. Triglyceride with medium-chain fatty acids increases the activity and expression of hormone-sensitive lipase in white adipose tissue of C57BL/6J mice. *Biosci Biotechnol Biochem* 2011; 75: 1939-1944.
- [31] Deng J, Liu S, Zou L, Xu C, Geng B, Xu G. Lipolysis response to endoplasmic reticulum stress in adipose cells. *J Biol Chem* 2012; 287: 6240-6249.
- [32] Ronti T, Lupattelli G, Mannarino E. The endocrine function of adipose tissue: an update. *Clin Endocrinol (Oxf)* 2006; 64: 355-365.
- [33] Alfaro-Moreno E, Martínez L, García-Cuellar C, Bonner JC, Murray JC, Rosas I, Rosales SP, Osornio-Vargas AR. Biologic effects induced in vitro by PM10 from three different zones of Mexico City. *Environ Health Perspect* 2002; 110: 715-720.
- [34] Soukup JM, Becker S. Human alveolar macrophage responses to air pollution particulates are associated with insoluble components of coarse material, including particulate endotoxin. *Toxicol Appl Pharmacol* 2001; 171: 20-26.
- [35] Brook RD, Jerrett M, Brook JR, Bard RL, Finkelstein MM. The relationship between diabetes mellitus and traffic-related air pollution. *J Occup Environ Med* 2008; 50: 32-38.
- [36] Pearson JF, Bachireddy C, Shyamprasad S, Goldfine AB, Brownstein JS. Association between fine particulate matter and diabetes prevalence in the U.S. *Diabetes Care* 2010; 33: 2196-2201.
- [37] Zhang K. Integration of ER stress, oxidative stress and the inflammatory response in health and disease. *Int J Clin Exp Med* 2010; 3: 33-40.

PM_{2.5} induces unfolded protein response

Supplemental Information
Sequences of real-time PCR primers

Gene	Forward primer	Reverse primer
Xbp1(s)	GAGTCCGCAGCAGGTG	GTGTCAGAGTCCATGGGA
Der11	CATCACGCGCTACTGGTTTG	CTTGCCGATCAAGGGGACAG
Edem1	TGGAATTTGGGATTCTGAGC	CTGCAGTCCAGGGAAGAAAAG
Acaca	GATGAACCATCTCCGTTGGC	CCCAATTATGAATCGGGAGTGC
Smaf1	TCTACCAGGTACCATCTGGGC	GTTTGGCAAGAGGCTTGGC
Ceacam1	CAAGTCACCAACACCACAGTC	TCTGAGGATGCTGTTGTTCTG
Plin1	CTGTGTGCAATGCCTATGAGA	CTGGAGGGTATTGAAGAGCCG
Dgat2	TTCCTGGCATAAGGCCCTATT	AGTCTATGGTGTCTCGGTTGAC
Fit2	GCCTCAAGGACACTCTCTGG	AACAACCATCCAGGCACTTC
Fsp27	AGCTAGCCCTTTCCCAGAAG	CCTTGTAGCAGTGCAGGTCA
Fat/Cd36	TTCACGGGCGTCCAGAA	GATCTTGCTGAGTCCGTTCCA
β-actin	GATCTGGCACCACACCTTCT	GGGGTGTGAAGGTCTCAA
Adipsin	TACATGGCTTCCGTGCAAGTG	CACAGAGTCGTCATCCGTC